Article

Sensitive and Selective Ratiometric Fluorescence Probes for Detection of Intracellular Endogenous Monoamine Oxidase A

Xiaofeng Wu, Lihong Li, Wen Shi, Qiuyu Gong, Xiaohua Li, and Huimin Ma

Just Accepted

Sensitive and Selective Ratiometric Fluorescence Probes for Detection of Intracellular Endogenous Monoamine Oxidase A

Xiaofeng Wu , Lihong Li, Wen Shi, Qiuyu Gong, Xiaohua Li, and Huimin Ma*

Beijing National Laboratory for Molecular Sciences, Key Laboratory of Analytical Chemistry for Living Biosystems, Institute of Chemistry, Chinese Academy of Sciences, Beijing 100190, China. E-mail: mahm@iccas.ac.cn

1

Abstract

Monoamine oxidase A (MAO-A) is known to widely exist in most cell lines in the body, and its dysfunction (unusually high or low levels of MAO-A) is thought to be responsible for several psychiatric and neurological disorders. Thus, a sensitive and selective method for evaluating the relative MAO-A levels in different live cells is urgently needed to better understand the function of MAO-A, but such a method is still lacking to our knowledge. Herein, we rationally design two new ratiometric fluorescence probes (**1** and **2**) that can detect MAO-A sensitively and selectively. The probes are constructed by incorporating a recognition group of propylamine into the fluorescent skeleton of 1,8-naphthalimide, and the detection mechanism is based on the amine oxidation and *β*-elimination to release the fluorophore (4-hydroxy-*N*-butyl-1,8-naphthalimide), which is verified by HPLC analysis. Reaction of the probes with MAO-A produces a remarkable fluorescence change from blue to green, and the ratio of fluorescence intensity at 550 and 454 nm is directly proportional to the concentration of MAO-A in the ranges of 0.5-1.5 μg/mL and 0.5-2.5 μg/mL, with detection limits of 1.1 ng/mL and 10 ng/mL (k = 3) for probe **1** and probe **2**, respectively. Surprisingly, these probes show strong fluorescence responses to MAO-A but almost not to MAO-B (one of two isoforms of MAO), indicating superior ability to distinguish MAO-A from MAO-B. The high specificity of the probes for MAO-A over MAO-B is further supported by different inhibitor experiments. Moreover, probe **1** displays higher sensitivity than probe **2**, and is thus investigated to image the relative MAO-A levels in different live cells such as HeLa and NIH-3T3 cells. It is found that the concentration of endogenous MAO-A in HeLa cells is about 1.8 times higher than that in NIH-3T3 cells, which is validated by the result from ELISA kit. In addition, the proposed probes may find more uses in the specific detection of MAO-A between the two isoforms of MAO, thereby promoting our understanding of behavior and function of MAO-A in living biosystems.

2

■ INTRODUCTION

Monoamine oxidases (MAO), a family of flavoenzymes that exist widely in most cell types in the body, can catalyze the oxidation of monoamines to the corresponding reaction products of aldehydes, hydrogen peroxide and ammonia/substituted amines.[1,2] Because of being encoded by distinct genes, MAO has two different types: MAO-A and MAO-B.[3-5] Both of them are vital to the inactivation of monoaminergic neurotransmitters, but display different specificities: MAO-A mainly breaks down serotonin, melatonin, noradrenaline, and adrenaline, whereas MAO-B mainly breaks down phenethylamine and benzylamine.[6-8] Moreover, MAO dysfunction (excessive or deficient levels of MAO) is thought to be responsible for several psychiatric and neurological disorders.[3,8-12] Therefore, much attention has been paid to the detection of MAO, and a number of methods including enzyme-linked immunosorbent assay (ELISA) and ^{19}F magnetic resonance have been developed to detect MAO in different biosystems.[13-16] For the assay of MAO in living cells, fluorescent probes combined with confocal imaging technique have some unique advantages such as high sensitivity, and great temporal and spatial sampling capability.[17-19] To the best of our knowledge, however, current fluorescent probes available are only suitable for the assay of either MAO-B or the total content of the two MAO isoforms,[18-26] and a fluorescent probe for the selective detection of MAO-A is still lacking. Obviously, developing a specific MAO-A fluorescent probe is rather necessary to promote better understanding of biological function of MAO-A.

In the present work, we have designed two new ratiometric fluorescence probes (**1** and **2;** Scheme 1) by using propylamine as a recognition moiety and 1,8-naphthalimide as an

excellent fluorescence moiety (tunable electronic system, good stability and cell-permeable

ability). We chose the skeleton of 1,8-naphthalimide, because its derivatives usually

produce a ratiometric fluorescence response,[27-29] which is beneficial to avoiding the

influence of several variants such as probe concentration and optical path length.[30-37] The

detection mechanism is based on the amine oxidation and β-elimination to release the

fluorophore (4-hydroxy-*N*-butyl-1,8-naphthalimide; NIOH, Scheme 1). The as-prepared

two probes displayed remarkable ratiometric fluorescence response to MAO-A rather than

MAO-B, indicating their superior ability to distinguish MAO-A from MAO-B. Moreover,

probe **1**, showing higher sensitivity than probe **2**, has been successfully used to image the

relative levels of endogenous MAO-A in different live cells.

Scheme 1. Synthesis of probes and their reaction with MAO.
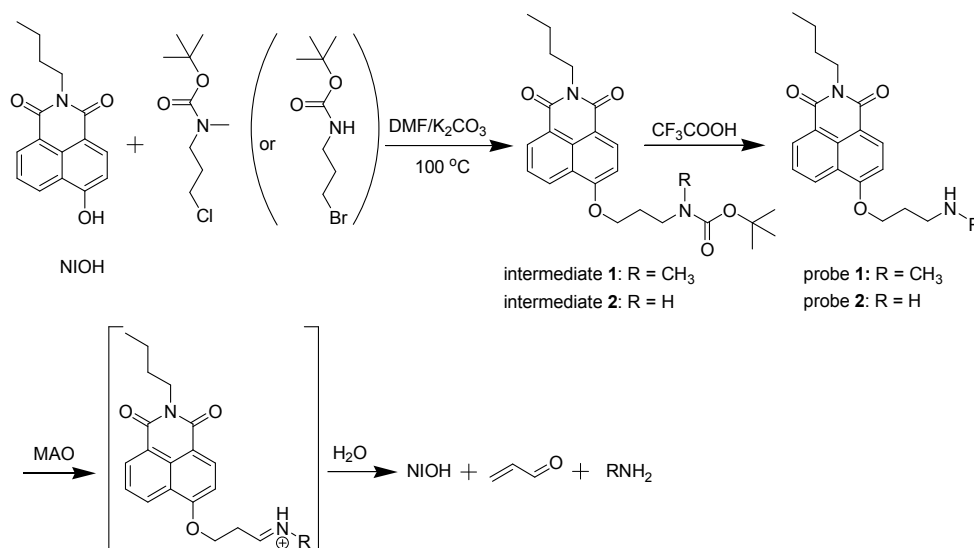
■ **EXPERIMENTAL SECTION**

Reagents. MAO-A, MAO-B, tryosinase, leucine aminopeptidase, carboxylesterase,

4-bromo-1,8-naphthalic anhydride, *N,N*-dimethylformamide (DMF, anhydrous), dimethyl

sulphoxide (DMSO), clorgyline, pargyline, and 3-(4,5-dimethyl-2-thiazolyl)-2,5-diphenyl-2H-tetrazolium bromide (MTT) were purchased from Sigma-Aldrich. n-butylamine, sodium methoxide, hydriodic acid (57%, w/v), 3-(BOC-amino)propyl bromide, trifluoroacetic acid, and N-BOC-N-methyl-3-chloro-1-propanamine were obtained from Beijing InnoChem Science & Technology Co., Ltd. Dichloromethane (superdry) was purchased from J&K Scientific Ltd. KCl, $MgCl_2$, $FeCl_3$, K_2CO_3, $ZnSO_4$ and $CuSO_4$ were obtained from Beijing Chemicals, Ltd. Phosphate buffered saline (PBS, 155.2 mM NaCl, 2.97 mM Na_2HPO_4, 1.05 mM KH_2PO_4; pH 7.4) solution was purchased from Invitrogen, and ELISA kit for MAO-A from Shanghai Jianglai Biotech Co., Ltd. RIPA lysis buffer (CW2333) was purchased from CoWin Bioscience, Inc. The cells lines (HeLa and NIH-3T3) and Dulbecco's modified Eagle's medium (DMEM) were obtained from KeyGEN BioTECH Co. LTD, Nanjing, China. The stock solution (1 mM) of probe **1** or **2** was prepared in DMSO. Ultrapure water (over 18 MΩ·cm) was used throughout.

Apparatus. ^{1}H-NMR and ^{13}C-NMR spectra were recorded on a Brucker DMX-300, DMX-400, or JEOL JNM-ECX 400 spectrometer. Electrospray ionization mass spectra (ESI-MS) were implemented with a Shimadzu LC-MS 2010A instrument (Kyoto, Japan). High-resolution electrospray ionization mass spectrometry (HR-ESI-MS) was performed on an APEX IVFTMS instrument (Bruker, Daltonics). Electron impact time-of-flight mass spectra (EI-TOF MS) and high resolution EI-TOF mass spectra (HR-EI-TOF MS) were recorded with a GCT mass spectrometer (Micromass, Manchester, UK). High-performed liquid chromatography (HPLC) analyses were conducted as described previously.[38] Absorption spectra were recorded with a TU-1900 spectrophotometer (Beijing, China) in

1-cm quartz cells. Fluorescence spectra were measured on a Hitachi F-4600 spectrofluorimeter in 1×1 cm quartz cells with both excitation and emission slit widths of 10 nm. The absorbance for MTT analysis and for the ELISA assay kit was recorded on a microplate reader (Molecular Devices SpectraMax i3). Fluorescence imaging was conducted on an FV 1200-IX83 confocal laser scanning microscope (Olympus, Japan), with an excitation wavelength of 405 nm and an optical section of 0.5 μm. The incubation was performed in a Shaker incubator (SKY-100C, China).

Syntheses of Probes 1 and 2. The starting material of NIOH was prepared following the reported procedure (see Scheme S1 in the Supporting Information for details; note that, in addition to ^{1}H-NMR spectra and mass spectral data, ^{13}C-NMR spectra were also provided for NIOH and its precursors NI-Br and NI-OCH$_3$).[29] Then, probes **1** and **2** were synthesized according to the route shown in Scheme 1.

Synthesis of Intermediate 1. To a solution of NIOH (0.081 g, 0.3 mmol) in 5 mL anhydrous DMF, K$_2$CO$_3$ (0.083 g, 0.6 mmol) was added with stirring under Ar atmosphere. Then, a solution of *N*-BOC-*N*-methyl-3-chloro-1-propanamine (0.075 g, 0.36 mmol) in DMF (1 mL) was added dropwise. The mixture was heated to 100 °C. After stirring at 100 °C for 48 h, the solution was cooled and diluted with dichloromethane (10 mL). The resulting solution was then washed with brine water (20 mL×3). The organic layer was separated and dried over anhydrous Na$_2$SO$_4$. The solvent was removed by evaporation under reduced pressure, and the residue was purified using silica gel chromatography with CH$_2$Cl$_2$/MeOH (v/v, 200:1 to 50:1) as eluent, obtaining intermediate **1** as a gray-white solid (0.078 g, yield 58%). ^{1}H-NMR and ^{13}C-NMR spectra of intermediate **1** are shown in

Figures S7 and S8 in the Supporting Information, respectively. ^{1}H-NMR (300 MHz, 298 K,

CD_3Cl): δ 8.60 (d, 1H, J=7.2 Hz), 8.56 (d, 1H, J=8.7 Hz), 8.53 (d, 1H, J=8.4 Hz), 7.69 (t,

1H, J=7.5 Hz), 7.02 (d, 1H, J=7.2 Hz), 4.29 (t, 2H, 6.3 Hz), 4.15 (t, 1H, J=7.5 Hz), 3.53 (t,

2H, J=6.6 Hz), 2.92 (s, 3H), 2.22-2.16 (m, 2H), 1.75-1.60 (m, 2H), 1.50-1.39 (m, 2H), 1.39

(s, 9H), 0.96 (t, 3H, J=7.2 Hz). ^{13}C-NMR (100 MHz, 298 K, CD_3Cl): δ 164.3, 163.8, 159.8,

155.8, 133.2, 131.5, 129.5, 128.4, 125.6, 123.8, 122.7, 115.1, 105.7, 79.5, 66.8, 45.9, 39.9,

30.3, 29.7, 28.5, 27.8, 20.4, 13.7. HR-ESI-MS: *m/z* calcd for intermediate **1**

($C_{25}H_{32}N_2NaO_5^+$, $[M+Na]^+$), 463.2203; found, 463.2206.

Synthesis of Intermediate 2. Intermediate **2**, prepared similarly as intermediate **1** using

NIOH and 3-(BOC-amino)propyl bromide, was obtained as a gray-white solid (0.090 g,

yield 70%). ^{1}H-NMR and ^{13}C-NMR spectra of intermediate **2** are shown in Figures S9 and

S10 in the Supporting Information, respectively. ^{1}H-NMR (300 MHz, 298 K, CD_3Cl): δ

8.59 (d, 1H, J=7.2 Hz), 8.54 (d, 1H, J=6.6 Hz), 8.52 (d, 1H, J=7.8 Hz), 7.71 (t, 1H, J=7.8

Hz), 7.02 (d, 1H, J=8.4 Hz), 4.83 (s, 2H), 4.35 (t, 2H, J=6 Hz), 4.18 (t, 2H, J=7.5 Hz),

3.48-3.42 (m, 2H), 2.20-2.16 (m, 2H), 2.20-2.16 (m, 2H), 1.75-1.65 (m, 2H), 1.50-1.38 (m,

2H), 1.43 (s, 9H), 0.97 (t, 3H, 7.2 Hz). ^{13}C-NMR (100 MHz, 298 K, CD_3Cl): δ 164.5,

163.8, 160.0, 156.0, 133.5, 131.7, 129.1, 128.7, 126.2, 123.4, 122.5, 115.1, 105.7, 79.3,

67.1 40.2, 38.0, 30.4, 29.7, 28.5, 20.5, 13.7. HR-ESI-MS: *m/z* calcd for intermediate **2**

($C_{24}H_{30}N_2NaO_5^+$, $[M+Na]^+$), 449.2047; found, 449.2046.

Synthesis of Probe 1. To a solution of intermediate **1** (0.044 g, 0.1 mmol) in anhydrous

CH_2Cl_2 (2 mL) at 0 °C, a solution of trifluoroacetic acid (0.75 mL) in anhydrous CH_2Cl_2 (1

mL) was added dropwise. The resulting mixture was stirred at 0 °C for 1 h, and then the

solvent was removed by evaporation under reduced pressure. The residue was subjected to silica chromatography with CH_2Cl_2/MeOH (v/v, 100:1 to 5:1) as eluent, obtaining probe **1** as a yellowish solid (0.031 g, yield 90%). ^{1}H-NMR and ^{13}C-NMR spectra of probe **1** are shown in Figures S11 and S12 in the Supporting Information, respectively. ^{1}H-NMR (300 MHz, 298 K, CD_3Cl): δ 8.54 (d, 1H, J=6.9 Hz), 8.46 (d, 1H, J=8.1 Hz), 8.44 (d, 1H, J=7.2 Hz), 7.66 (t, 1H, 7.8 Hz), 6.97 (d, 1H, J=8.4 Hz), 4.35 (t, 1H, J=5.7 Hz), 4.13 (t, 2H, J=7.2 Hz), 3.27 (t, 2H, J=7.2 Hz), 2.76 (s, 3H), 2.53- 2.49 (m, 2H), 1.74-1.64 (m, 2H), 1.50-1.34 (m, 2H), 0.97 (t, 3H, J=7.2 Hz). ^{13}C-NMR (100 MHz, 298 K, CD_3Cl): δ 164.2, 163.6, 159.0, 133.0, 131.4, 129.1, 128.0, 126.0, 123.0, 122.4, 115.5, 105.8, 65.6, 47.0, 40.1, 33.6, 30.2, 26.3, 20.4, 13.9. HR-ESI-MS: *m/z* calcd for probe **1** ($C_{20}H_{25}N_2O_3^+$, $[M+H]^+$), 341.1860; found, 341.1856.

Synthesis of Probe 2. Probe **2**, prepared similarly as probe **1** using intermediate **2** and trifluoroacetic acid, was obtained as a yellowish solid (0.029 g, yield 88%). ^{1}H-NMR and ^{13}C-NMR spectra of probe **2** are shown in Figures S13 and S14 in the Supporting Information, respectively. ^{1}H-NMR (400 MHz, 298 K, DMSO-d_6): δ 8.49 (d, 1H, J=12 Hz), 8.43 (d, 1H, J=8 Hz), 8.38 (d, 1H, J=8 Hz), 7.75 (d, 1H, J=8 Hz), 7.25 (d, 1H, J=8 Hz), 4.37 (t, 2H, J=8 Hz), 4.00 (t, 2H, J=8 Hz), 2.92 (t, 2H, J=8 Hz), 2.09-2.03 (m, 2H), 1.62-1.54 (m, 2H), 1.38-1.29 (m, 2H), 0.91 (t, 3H, J=8 Hz). ^{13}C-NMR (100 MHz, 298 K, DMSO-d_6): δ 164.0, 163.3, 160.1, 133.6, 131.4, 1290, 128.7, 126.7, 123.3, 122.3, 114.5, 107.3, 67.1, 40.5, 38.0, 30.8, 30.2, 20.3, 14.2. HR-ESI-MS: *m/z* calcd for probe **2** ($C_{19}H_{23}N_2O_3^+$, $[M+H]^+$), 327.1703; found, 327.1670.

Modeling of the Binding Affinity between Probe 1 and MAO-A (or MAO-B). The binding affinity between probe **1** and MAO-A (or MAO-B) was estimated as described previously.[38] The crystal structure of MAO-A (or MAO-B) complex was collected from PDB under code 2BXR (or code 1OJC).

General Procedure for MAO-A Detection. Unless otherwise specified, all the fluorescence measurements were made as follows. In a 5 mL test tube, 4 mL of PBS (pH 7.4) and 50 μL of the stock solution of probe **1** (or probe **2**) were mixed, followed by addition of an appropriate volume of MAO-A sample solution. The final volume was adjusted to 5 mL with PBS and the reaction solution was mixed well. After incubating for 4.5 h in a Shaker incubator at 37 °C, a 3-mL portion of the reaction solution was transferred to 1-cm quartz cell to measure absorbance at 450 nm and/or the ratio ($R = I_{550}/I_{454}$) of fluorescence intensity at $\lambda_{em} = 550$ nm and $\lambda_{em} = 454$ nm with $\lambda_{ex} = 425$ nm (both excitation and emission slit widths were set to 10 nm). Under the same conditions, a blank solution containing no MAO-A was prepared and measured for comparison.

Determination of Endogenous MAO-A in Cells by ELISA Kit. The cell lysate was first prepared according to the following procedure. In a test tube, 1×10^6 cells (HeLa or NIH-3T3) in 1 mL DMEM was centrifuged at 3000 rpm for 5 min, and then the supernatant was discarded, followed by washing the cells with PBS (2 mL×3). After discarding the PBS, 200 μL RIPA lysis buffer was added to the test tube, and the tube was left at 0 °C for 20 min. Then, the tube was centrifuged at 12000 rpm for 10 min, and the supernatant was collected for use.

The concentration of endogenous MAO-A in the cells was then determined by measuring the absorbance at 450 nm using a commercial MAO-A ELISA kit. In brief, the cell lysate (10 μL) and sample diluent (40 μL) were added to the ELISA kit wells containing solid-phase antibody. After incubation at 37 °C for 30 min, all the wells were washed five times with wash solution (300 μL). Then to each well (except the blank well), horseradish peroxidase-conjugate reagent (50 μL) was added. After incubation at 37 °C for 30 min, all the wells were washed five times with wash solution (300 μL) again, and then chromogen solution A (50 μL) and chromogen solution B (50 μL) were added to each well. The reaction mixture was incubated at 37 °C for 15 min in the dark. Finally, the stop solution (50 μL) was added to each well to stop the reaction, and read the absorbance at 450 nm within 15 min.[39,40] The concentrations of endogenous MAO-A in the corresponding cells were calculated according to the standard curve prepared following the direction of the kit. Data were expressed as mean ± standard deviation (SD) of three separate measurements.

Fluorescence Imaging of Endogenous MAO-A in HeLa and NIH-3T3 Cells. Cells (HeLa or NIH-3T3) were grown on the glass-bottom culture dishes (MatTek CO.) in DMEM supplemented with 10% (v/v) fetal bovine serum (FBS) and 1% (v/v) penicillin-streptomycin at 37 °C in a humidified 5% CO_2 incubator. Before use, the adherent cells were washed three times with FBS-free DMEM. For fluorescence imaging, the cells were incubated with 10 μM of probe **1** in FBS-free DMEM at 37 °C for 1 h, similar to our previous operation.[34]

Cytotoxicity Assay. The cytotoxicity of probe **1** to HeLa cells was evaluated by a standard MTT assay, as described previously.[34]

10

1
2
3
4
5
6
7
8
9
10
11
12
13
14
15
16
17
18
19
20
21
22
23
24
25
26
27
28
29
30
31
32
33
34
35
36
37
38
39
40
41
42
43
44
45
46
47
48
49
50
51
52
53
54
55
56
57
58
59
60

■ RESULTS AND DISCUSSION

Spectroscopic Properties of Probes 1 and 2. The absorption and fluorescence spectra of

probe **1** before and after reaction with MAO-A are shown in Figure 1. As seen from Figure

1A, probe **1** itself displays an absorption maximum at 374 nm, but its reaction solution with

MAO-A exhibits a strong absorption peak at about 450 nm, with a dramatic color change

from colorless to yellow (see the inset in Figure 1A). Fluorescence studies revealed that

probe **1** has an excitation and emission peak at 425 nm and 454 nm, respectively. Reaction

of probe **1** with MAO-A leads to a large decrease in the fluorescence intensity at 454 nm,

accompanied by the formation of a new red-shifted fluorescence peak at around 550 nm

(Figure 1B). This large shift, with a distinct color change from blue to green (the inset of

Figure 1B), leads to about 56-fold enhancement in the fluorescence intensity ratio (I_{550}/I_{454}).

Probe **2** shows a similar spectroscopic response to MAO-A, including absorption (Figure

S15A) and fluorescence (Figure S15B) change. The above results indicate that both of

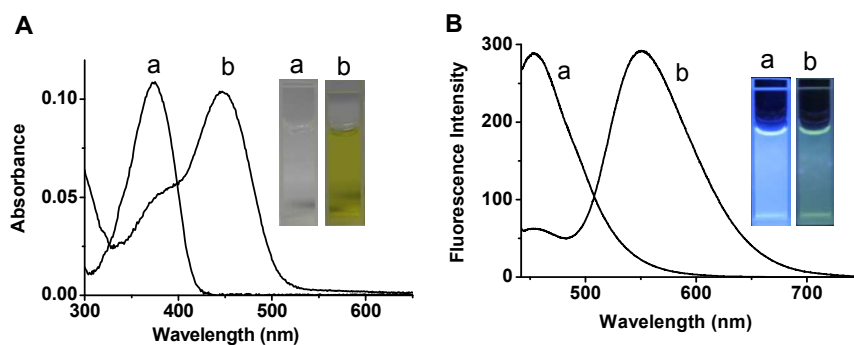fluorescence probes **1** and **2** can be used for the ratiometric detection of MAO-A.

Figure 1. (A) Absorption and (B) fluorescence emission spectra of probe **1** (10 μM) before

(a) and after (b) reaction with MAO-A (2 μg/mL) at 37 °C for 4.5 h in PBS (pH 7.4). λ_{ex} =

425 nm.

Specificity of the Probes for MAO-A over MAO-B. The specificity of the probes for

the two MAO isoforms was investigated under the same conditions. Theoretically, probe **1**

or probe **2** should produce fluorescence response to both of MAO-A and MAO-B, because

the two MAO isoforms have similar oxidation of monoamines. However, we were

surprised to find that these probes exhibit highly specific fluorescence response to MAO-A

over MAO-B. As shown in Figure 2, the fluorescence intensity ratio of probe **1** reacting

with MAO-A is about 200-fold higher than that with MAO-B; similarly, MAO-A caused a

much larger fluorescence increase (about 60-fold) of probe **2**, as compared with MAO-B.

These results indicate that both of probes **1** and **2** have superior ability to distinguish

MAO-A from MAO-B, and probe **1** displays better sensitivity than probe **2** (see also Figure

S16 in the Supporting Information for more comparisons). Thus, probe **1** was chosen in

further studies on the MAO-A assay.

   The reason of the two probes for the high specificity for MAO-A over MAO-B is unclear

and may be complex, but a possible explanation may be due to the fact that each enzyme

has its own specific substrate. To further explore this issue, we conducted a docking study[38]

so as to estimate the binding affinity between probe **1** and the two MAO isoforms. The

docking scores (-lgK_d) of probe **1** with MAO-A and MAO-B were found to be 7.31 and

4.38, respectively, indicating that MAO-A has a much stronger binding ability than

MAO-B. This result is supported by the ribbon model created by Pymol as well as the

active pocket model (Figure S17), from which it is seen that a potential hydrogen bond

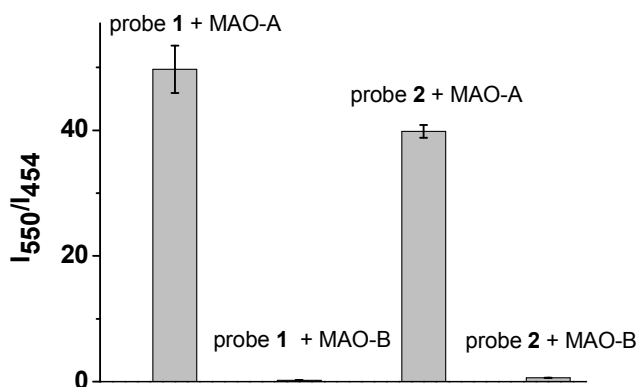exists between MAO-A and probe **1** (Figure S17c), but not between MAO-B and probe **1**.

Figure 2. The ratio changes of fluorescence intensity of probe **1** (10 μM) and probe **2** (10 μM) upon reaction with MAO-A (15 μg/mL) and MAO-B (15 μg/mL) for 4.5 h. λ_{ex} = 425 nm.

Reaction Conditions and Analytical Characteristics. Reaction conditions for probe **1** with MAO-A were optimized, including the effects of pH, temperature and time. As shown in Figure S18 in the Supporting Information, the ratio value of probe **1** itself is hardly affected by the change of either pH from 4.5 to 9.0 or temperature from 25 to 42.5 °C. However, introduction of MAO-A into the reaction system containing probe **1** leads to a large fluorescence enhancement in the range of pH 7.4-9 and temperature from 25 to 42.5 °C, indicating that this enzyme displays good activity under the physiological conditions. Fluorescence kinetic curves of probe **1** reacting with MAO-A at different concentrations are shown in Figure S19 (Supporting Information), which reveals that higher concentrations of MAO-A results in faster response and stronger fluorescence. For no more than 15 μg/mL MAO-A, the fluorescence can reach a plateau after about 4.5 h. In contrast, the fluorescence of probe **1** itself nearly keeps constant within 4.5 h, indicating its high stability in the detection system. Note that the reaction of MAO-B with its substrates is also slow,[19,24] which may result from the nature of MAO.

13

Figure 3 shows the fluorescence change of probe **1** reacting with MAO-A at varied

concentrations. As is seen, the fluorescence intensity gradually increases at 550 nm but

decreases at 454 nm with increasing the concentration of MAO-A, and a good linearity

between the fluorescence intensity ratio and the MAO-A concentration in the range of

0.5-1.5 μg/mL is observed, with an equation of $I_{550}/I_{454} = 1.97 \times [MAO-A] - 0.44$ (r = 0.994).

The detection limit $(k = 3)^{33}$ was determined to be 1.1 ng/mL, showing high sensitivity.

Similarly, probe **2** also displays a good linear fluorescence response to MAO-A in the

concentration range of 0.5-2.5 μg/mL (Figure S15C, Supporting Information), with an

equation of $I_{550}/I_{454} = 0.24 \times [MAO-A] - 0.022$ (r = 0.998) and a detection limit of 10 ng/mL.
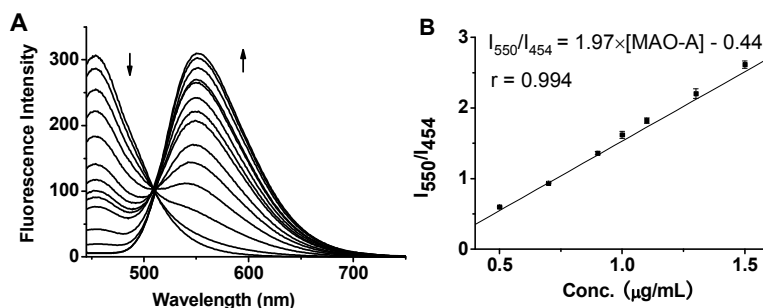

Figure 3. (A) Fluorescence response of probe **1** (10 μM) to MAO-A at different
concentrations (0, 0.1, 0.3, 0.5, 0.7, 0.9, 1.1, 1.3, 1.5, 1.7, 2.5, 4, 10, and 15 μg/mL). (B)
The Linear fitting curve between the fluorescence intensity ratio (I_{550}/I_{454}) and the
concentration of MAO-A. $\lambda_{ex} = 425$ nm.

The selectivity of the reaction was studied by examining various potential interfering

species in parallel under the same conditions, including inorganic salts (KCl, MgCl$_2$,

FeCl$_3$, ZnSO$_4$), glucose, vitamin C, vitamin B$_6$, H$_2$O$_2$, ariginine, serine, glutamic acid,

alanine, cysteine, glutathione, urea, creatinine, and some enzymes (carboxylesterase,

tyrosinase, leucine aminopeptidase). As depicted in Figure 4, probe **1** exhibits excellent

14

selectivity for MAO-A over the other species tested, which may be ascribed to the specific
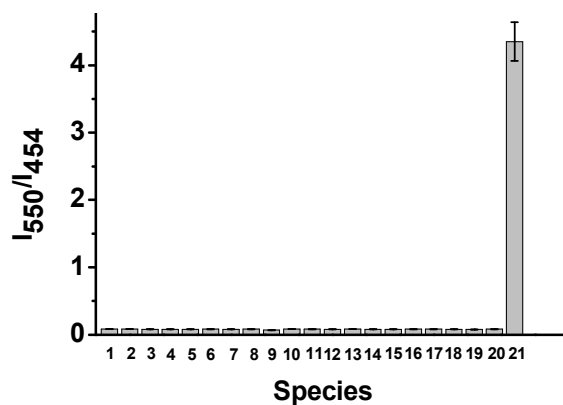
oxidation of the substrate by the enzyme.

Figure 4. Fluorescence response of probe **1** (10 μM) to various species. (1) blank; (2) KCl

(150 mM); (3) MgCl$_2$ (2.5 mM); (4) FeCl$_3$ (100 μM); (5) ZnSO$_4$ (100 μM); (6) glucose (10

mM); (7) vitamin B$_6$ (1 mM); (8) vitamin C (1 mM); (9) H$_2$O$_2$ (100 μM); (10) arginine (1

mM); (11) serine (1 mM); (12) glutamic acid (1 mM); (13) alanine (1 mM); (14) cysteine (1

mM); (15) glutathione (1 mM); (16) urea (20 mM); (17) creatinine (10 mM); (18)

carboxylesterase (1 mg/mL); (19) tyrosinase (0.5 U/mL); (20) leucine aminopeptidase (100

U/L); (21) MAO-A (2 μg/mL).

　Reaction Mechanism. The reaction products of probe **1** with MAO-A were analyzed

with ESI-MS and HPLC to investigate the spectroscopic response mechanism. As shown in

Figure S20 in the Supporting Information, the ESI-MS spectrum from the reaction solution

of probe **1** with MAO-A exhibits a major peak at m/z =268.1 [M-H]$^-$, indicating the release

of the fluorophore NIOH. Moreover, HPLC analyses further verified the generation of

NIOH as a reaction product. As shown in Figure S21 (Supporting Information), upon

reaction with MAO-A, the peak at 4.38 min representing probe **1** (curve A) decreases

significantly, accompanied by the appearance of a new peak at 8.98 min indicative of

NIOH (curve B). The above results clearly indicate that the fluorescence response results from the generation of NIOH (Scheme 1).

To prove the fluorescence change resulting from the action of MAO-A, the effect of the specific inhibitor, clorgyline,[1] on the enzyme activity was also examined. As shown in Figure S22 (Supporting Information), the fluorescence intensity ratio in the presence of 1 nM clorgyline is much less than that in the absence of the inhibitor, and more clorgyline (10 nM) causes larger decrease in the fluorescence intensity ratio. These results demonstrate that the fluorescence change of probe **1** in the presence of MAO-A indeed arises from the enzyme-catalyzed oxidation.

Cytotoxicity Assay. The potential toxicity of probe **1** to cells was evaluated by a standard MTT assay (Figure S23 in the Supporting Information). The results showed that the cell viability was not significantly affected upon treatment with probe **1** up to 10 μM at 37 °C for 24 h, suggesting the low cytotoxicity and good biocompatibility of probe **1**.

Fluorescence Imaging of Relative Levels of Endogenous MAO-A in Different Cells. Probe **1** is anticipated to detect the relative levels of endogenous MAO-A in different cells via confocal fluorescence imaging, and HeLa and NIH-3T3 cells were employed to investigate this potential. Before doing so, the capability of probe **1** for imaging endogenous MAO-A in cells was first examined by different inhibitor experiments. As shown in Figure 5, HeLa cells themselves display rather weak background fluorescence (column a in Figure 5A; control). However, the cells treated with probe **1** exhibits a strong fluorescence (column b in Figure 5A), demonstrating the good cell-permeability of probe **1** and its possible reaction with MAO-A in the cells to generate fluorescence response (note

that almost no fluorescence is observed in cell nucleus). Moreover, a ratio value of $R = 0.25$ $\pm\ 0.01$ can be obtained from the ratio image in column b (see also Figure 5B). To verify the intracellular fluorescence response resulting from MAO-A, clorgyline (specific inhibitor of MAO-A) experiments were performed. It was found that the cells pretreated with 10 μM clorgyline produced a largely decreased R value of 0.16±0.01 (the ratio image in column c of Figure 5A; see also Figure 5B), and more clorgyline (40 μM) further decreased the R value to 0.087±0.002 (the ratio image in column d of Figure 5A; see also Figure 5B). On the other hand, an additional inhibitor experiment was made by pretreating the cells with pargyline[1] (specific inhibitor of MAO-B). As can be seen from column e in Figure 5A, no significant fluorescence change is found as compared to column b, and the corresponding R value ($R = 0.23\pm0.01$; see also Figure 5B) is rather close to $R = 0.25$ without any inhibitor. Furthermore, clorgyline and pargyline hardly affected the fluorescence of both probe **1** and its reaction product NIOH (Figure S24, Supporting Information). Based on the above observations, therefore, it may be concluded that the intracellular fluorescence change is attributed to the MAO-A action, and probe **1** is capable of imaging endogenous MAO-A instead of MAO-B in cells.
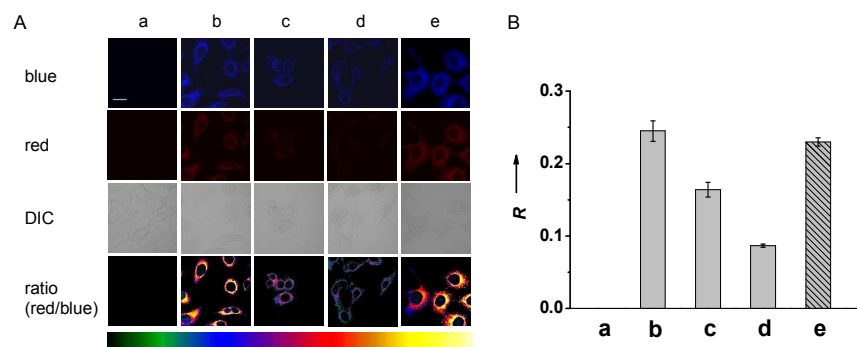
Figure 5. (A) Fluorescence images of HeLa cells. (a) Cells only (control); (b) the cells were incubated with probe **1** (10 μM) for 1 h; (c) the cells were pretreated with 10 μM clorgyline

(inhibitor of MAO-A) for 1.5 h, and then incubated with probe **1** (10 μM) for 1 h; (d) the cells were pretreated with 40 μM clorgyline for 1.5 h, and then incubated with probe **1** (10 μM) for 1 h; (e) the cells were pretreated with 40 μM pargyline (inhibitor of MAO-B) for 1.5 h, and then incubated with probe **1** (10 μM) for 1 h. The images of the first row (blue channel of probe **1**) and second row (red channel of NIOH) were collected in the ranges of 430-490 nm and 500-560 nm, respectively; the third row shows the corresponding differential interference contrast (DIC) images; the fourth row shows the ratio images generated by Olympus software (FV10-ASW); the bottom color strip represents the pseudocolor changes with MAO-A. Scale bar, 20 μm; λ_{ex} = 405 nm. (B) The relative fluorescence intensity ratio (R=$I_{500\text{-}560}$/$I_{430\text{-}490}$) generated by Olympus software according to the corresponding ratiometric images (i.e., the fourth row in Figure 5A) of HeLa cells. The R values were obtained from triplicate experiments (n=3).

Having demonstrated the high specificity for MAO-A, probe **1** was then used to detect the relative MAO-A levels in different cells under the same fluorescence imaging conditions. As shown in Figure 6A, HeLa cells generate stronger fluorescence than NIH-3T3 cells (compare the corresponding two ratio images), and the fluorescence intensity ratio from HeLa is about 1.8 times higher than that from NIH-3T3 (Figure 6B), which indicates that the MAO-A level in the two kinds of cells are different. Supposing that the reaction properties of probe **1** in the two cell lines are equal, the concentration/activity of MAO-A in HeLa cells would be about 1.8 times higher than that in NIH-3T3 cells, which provides the first semi-quantitative information about the MAO-A contents in these two cell lines. Moreover, the levels of MAO-A in the cells were determined by ELESA kit (Figure 6C), which reveals that the activity of MAO-A in HeLa cells is about 2 times higher than that in NIH-3T3 cells, clearly supporting the above results.
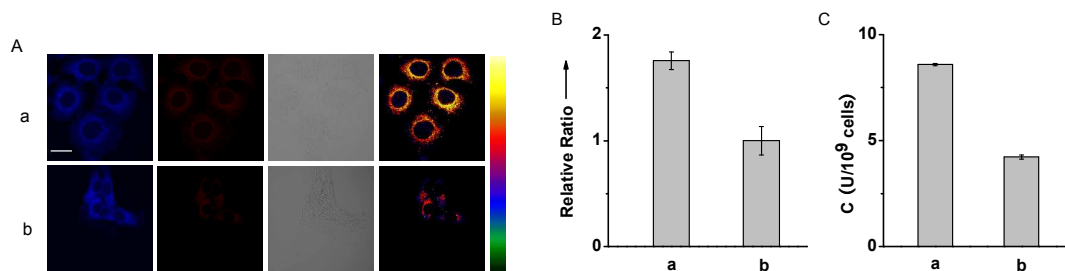
Figure 6. (A) Confocal fluorescence images of different cell lines. (a) HeLa; (b) NIH-3T3. The images of the first column (blue channel of probe **1**) and second column (red channel of NIOH) were collected in the ranges of 430-490 nm and 500-560 nm, respectively; the third column shows the corresponding DIC images; the fourth column shows the ratio images generated by Olympus software; the right color strip represents the pseudocolor changes with MAO-A. The cells were incubated with probe **1** (10 μM) at 37 °C for 1 h. Scale bar, 20 μm; λ_{ex} = 405 nm. (B) Relative ratio values from the corresponding ratio images in panel A (the ratio value from NIH-3T3 is defined as 1.0). (C) The activity of MAO-A in (a) HeLa and (b) NIH-3T3 cells determined by ELISA kit. The results are expressed as the mean ± standard deviation of three separate measurements.

■ CONCLUSIONS

In summary, by incorporating propylamine into the fluorescent skeleton of 1,8-naphthalimide, we have developed two new ratiometric fluorescence probes for the selective detection of MAO-A rather than MAO-B (the other isoform of MAO), of which probe **1** exhibits higher sensitivity with a detection limit of 1.1 ng/mL MAO-A. The high specificity of the probes for MAO-A over MAO-B is further supported by different inhibitor experiments. Moreover, with probe **1**, the relative levels of endogenous MAO-A in different cells such as HeLa and NIH-3T3 have been successfully detected via confocal fluorescence imaging, which reveals that the concentration of MAO-A in HeLa cells is about 2 times higher than that in NIH-3T3 cells. Most notably, this result has been

19

validated by ELISA kit. The excellent analytical performance of probe **1** makes it useful to

selectively detect MAO-A in various biosystems.

■ AUTHOR INFORMATION

Corresponding Author

*E-mail: mahm@iccas.ac.cn. Phone: +86-10-62554673.

■ ACKNOWLEDGMENT

■ ASSOCIATED CONTENT

Supporting Information

Additional information, as noted in the text. This material is available free of charge *via* the Internet at http://pubs.acs.org.

■ REFERENCES

(1)   Youdim, M. B.; Edmondson, D.; Tipton, K. F. *Nat. Rev. Nurosci.* **2006,** *7,* 295-309.

(2)   Berry, M. D.; Juorio, A. V.; Paterson, I. V. *Prog. Neuroboil.* **1994,** *42***,** 375-391.

(3)   Edmondoson, D. E.; Binda, C.; Wang, J.; Upadhyay, A. K.; Mattevi, A.
Biochemistry **2009,** *48,* 4420-4430.

(4)   Bortalato, M.; Godar, S. C.; Tambaro, S.; Li, F. G.; Devoto, P.; Coba, M. P.; Chen, K.; Shih, J.C. *Neuropharmacology* **2013,** *75,* 23-232.

(5)   Wang, C. C.; Billett, E.; Borchert, A.; Kuhn, H.; Ufer, C. *Cell. Mol. Life Sci.* **2013,** *70,* 599-630.

(6)   Prada, M. D.; Kettler, R.; Keller, H. H.; Cesura, A. M.; Richards, J. G.; Marti, J. S.;

Muggli-Maniglio, D.; Wyss, P. C.; Kyburz, E.; Imhof, R. *J. Neural. Transm.* **1990.**

29, 279-292.

(7)   Silverman, R. B. *Acc. Chem. Res.* **1995,** *28,* 335-342.

(8)   Brunner, H. G.; Nelen, M.; Breakfeild, X. O.; Ropers, H. H.; Van Oost, B. A.

Science **1993,** *262,* 578-580.

(9)   Choi, J. W.; Jang, B. K.; Cho, N. C.; Park, J. H.; Yeon, S. K.; Ju, E. J.; Lee, Y. S.;

Han, G.; Pae, A. N.; Kim, D. J.; Park, K. D. *Bioorg. Med. Chem.* **2015,** *23,*

6486-6496.

(10)   Satram-Maharaj, T.; Nyarko, J. N. K.; Kuski, K.; Fehr, K.; Pennington, P. R.; Truitt,

L.; Freywald, A.; Lukong, K. E.; Anderson, D. H. Mousseau, D. D. *Cellular*

Signalling **2014,** *26,* 2621-2632.

(11)   Tzvetkov, N. T.; Hinz, S.; Küppers, P.; Gastreich, M.; Müller, C. E. *J. Med. Chem.*

2014, *57,* 6679-6703.

(12)   Silver, R. B.; Zhou, J. J. P.; Ding, C. Z.; Lu, X. L. *J. Am. Chem. Soc.* **1995,** *117,*

12895-12896.

(13)   Krajl, M. *Biochem. Pharmacol.* **1965,** *14,* 16-1686.

(14)   Zhou, J. J. P.; Zhong, B. Y.; Silverman, R. B. *Anal. Biochem.* **1996,** *234,* 9-12.

(15)   Zhou, M. J.; Panchuk-Voloshina, N. *Anal. Biochem.* **1997,** *253,* 169-174.

(16)   Yamaguchi, K.; Ueki, R.; Nonaka, H.; Sugiraha, F.; Matasuda, T.; Sando, S. *J. Am.*

Chem. Soc. **2011,** *133,* 14208-14211.

(17)   Li, X. H.; Gao, X. H.; Shi, W.; Ma, H. M. *Chem. Rev.* **2014,** *114,* 590-659.

(18)   Li, X. F.; Zhang, H. T. Xie, Y. S.; Hu, Y.; Sun, H. Y.; Zhu, Q. *Org. Biomol. Chem.*

2014, *12,* 2033-2036.

(19) Li, L.; Zhang, C. W.; Chen, G. J.; Zhu, B. W.; Chai, C.; Xu, Q. H.; Tan, E. K.; Zhu, Q.; Lim, K. L.; Yao, S. Q. *Nat. Commun.* **2014,** *5*, 3276.

(20) Chen, G.; Yee, D. J.; Gubernator, N. G.; Sames, D. *J. Am. Chem. Soc.* **2005**, *127,* 4544-4545.

(21) Albers, A. E.; Rawls, K. A.; Chang, C. J. *Chem. Commun.* **2007,** 4647-4649.

(22) Li, L.; Zhang, C. W.; Ge, J. Y.; Qian, L. H.; Chai, B. H.; Zhu, Q.; Lee, J. S.; Lee, K. L.; Yao, S. Q. *Angew. Chem. Int. Ed.* **2015,** *54,* 1-6.

(23) Kim, D.; Sambasivan, S.; Nam, H.; Kim, K. H.; Kim, J. Y.; Joo, T.; Lee, K. H.; Kim, K. T.; Ahn, K. H. *Chem. Commun.* **2012,** *48,* 6833-6835.

(24) Long, S. B.; Chen, L.; Xiang, Y. M.; Song, M. G.; Zheng, Y. G.; Zhu, Q. *Chem. Commun.* **2012**, *48,* 7164-7166.

(25) Zhou, W. H.; Valley, M. P.; Shultz, J.; Hawkins, E. M.; Bernad, L.; Good, T.; Good, D.; Riss, T. L.; Klaubert, D. H.; Wood, K. W. *J. Am. Chem. Soc.* **2006,** *128,* 3122-3123.

(26) Peng, L. H.; Zhang G. X.; Zhang, D. Q.; Wang, Y. L.; Zhu, D. B. *Analyst* **2010,** *135,* 1779-1784.

(27) Zhu, B. C.; Gao, C. C; Zhao, Y. Z.; Liu, C. Y.; Li, Y. M.; Wei, Q.; Ma, Z. M.; Du, B.; Zhang, X. L. *Chem. Commun.* **2011,** *47,* 8656-8658.

(28) Liu, C. Y.; Wu, H. F.; Wang, Z. K.; Shao, C. X.; Zhu, B. C.; Zhang, X. L. *Chem. Commun.* **2014,** *50,* 6013-6016.

(29) Ren, Y.; Wu, Z.; Zhou, Y.; Li, Y.; Xu, Z. X. *Dyes Pigm.* **2011,** *91,* 442-445.

(30) Yan, X.; Li, H. X.; Zheng, W. S.; Su, X. G. *Anal. Chem.* **2015,** *87,* 8904-8909.

(31)   Teng, Y.; Jia, X. F.; Li, J.; Wang, E. K. *Anal. Chem.* **2015,** *87,* 4897-4902.

(32)   Wen, Y.; Liu, K. Y.; Yang, H. R.; Li, Y.; Lan, H. C.; Liu, Y.; Zhang, X. Y.; Yi, T. *Anal. Chem.* **2014,** *86,* 9970-9976.

(33)   Wan, Q. Q.; Song, Y. C.; Li, Z.; Gao, X. H.; Ma, H. M. *Chem. Commun.* **2013,** *49,* 502-504.

(34)   Wan, Q. Q.; Chen, S. M.; Shi, W.; Li, L. H.; Ma, H. M. *Angew. Chem. Int. Ed.* **2014,** *53,* 10916-10920.

(35)   Yuan, L.; Lin, W. Y.; Zheng, K. B.; Zhu, S. S. *Acc. Chem. Res.* **2013,** *46,* 1462-1473.

(36)   Chen, H.; Lin, W. Y.; Jiang, W. Q.; Dong, B. L.; Cui, H. J.; Tang, Y. H. *Chem. Commun.* **2015,** *51,* 6968-6971.

(37)   He, L. W.; Lin, W. Y.; Xu, Q. Y.; Wei, H. P. *Chem. Commun.* **2015,** *51,* 1510-1513.

(38)   Li, L. H.; Li, Z.; Shi, W.; Li, X. H.; Ma, H. M. *Anal. Chem.* **2014,** *86,* 6115-6120.

(39)   Wang, Z.; Li, X. H.; Song, Y. C.; Li, L. H.; Shi, W.; Ma, H. M. *Anal. Chem.* **2015,** *87,* 5816-5823.

(40)   Wang, Z.; Li, X. H.; Feng, D.; Li, L. H.; Shi, W.; Ma, H. M. *Anal. Chem.* **2014,** *86,* 7719-7725.

For TOC only